Published in final edited form as:

Muscle Nerve. 2020 December ; 62(6): 757–761. doi:10.1002/mus.27061.

Muscle phenotype of a rat model of Duchenne muscular dystrophy

Shama R. Iyer, PhD[1], **Su Xu, PhD**[2], **Sameer B. Shah, PhD**[3], **Richard M. Lovering, PhD, PT**[1]

[1]Department of Orthopaedics, University of Maryland School of Medicine, Baltimore, Maryland [2]Department of Diagnostic Radiology and Nuclear Medicine, University of Maryland School of Medicine, Baltimore, Maryland [3]Departments of Orthopaedic Surgery and Bioengineering, University of California San Diego, La Jolla, California

Abstract

Introduction: Our aim was to assess key muscle imaging and contractility parameters in the Duchenne muscular dystrophy (DMD) rat model (Dmd-KO rat), which have not yet been characterized sufficiently.

Methods: We performed in-vivo magnetic resonance imaging (MRI) for thigh and leg muscles, and performed hematoxylin and eosin (H&E) staining and in-vivo muscle contractility testing in specific hindlimb muscles.

Results: MRI prior to testing muscle contractility revealed multiple, unevenly distributed focal hyperintensities in the Dmd-KO rat quadriceps and tibialis anterior muscles. H&E staining showed corresponding areas of inflammation and ongoing regeneration. In-vivo contractile testing showed maximal force generated by Dmd-KO muscles was significantly lower, and susceptibility to injury was ~ two-fold greater in the Dmd-KO rats compared to wild-type (WT) rats.

Discussion: Together, the MRI findings, histological findings, and the low strength and high susceptibility to injury in muscles support use of the Dmd-KO rat as an animal model of DMD.

Keywords

Dmd-KO rat; eccentric injury; MRI; muscular dystrophy; skeletal muscle

1 | INTRODUCTION

Duchenne muscular dystrophy (DMD) is an X-linked muscle disorder caused by the absence of dystrophin, a large membrane-associated protein expressed in striated muscle. DMD is

Correspondence: Richard M. Lovering, School of Medicine, Department of Orthopaedics, University of Maryland, 685 W. Baltimore St., Baltimore, MD 21201. rlovering@som.umaryland.edu.

CONFLICT OF INTEREST

None of the authors has any conflict of interest to disclose.

ETHICAL PUBLICATION

We confirm that we have read the Journal's position on issues involved in ethical publication and affirm that this report is consistent with those guidelines.

characterized clinically by severe, progressive muscle degeneration and ongoing loss of muscle function.[1–3]

Much of what is known about dystrophin's functions is derived from studies of the *mdx* mouse. Similar to patients with DMD, dystrophin is missing from all muscle tissues in the *mdx* mouse. The *mdx* mouse has a peak in muscle weakness, necrosis, and regeneration between the second and fifth week of life ("critical period").[4–7] However, compared to the clinical course of patients with DMD, the phenotype is mild in the *mdx* mouse, showing some resolution of muscle damage after the critical period and a lifespan that is similar to the healthy, wild-type (WT) mouse. Therefore, the validity of the *mdx* mouse as a model of DMD is disputable.[8]

Recently, rat models of DMD have been generated.[9,10] These animals lack dystrophin, but unlike *mdx* mice, the rat models of DMD show severe muscle fibrosis and fatty infiltration, and have cardiac dysfunction and overall decreased activity. Thus, rat models of DMD could be useful for DMD pre-clinical research.[11] The larger size of the rat provides many advantages over the mouse, and the patterns of progressive muscle degeneration with age better mimic those observed in DMD than the *mdx* mouse. However, newly developed rat models have yet to be sufficiently described, especially with regard to assessment of muscle contractile function, making their use as experimental models uncertain.[12] The primary purpose here was to rigorously test in-vivo strength (maximal isometric torque) and susceptibility to injury (loss of strength after injury) using established methods that do not rely on behavior or volition in an awake animal. We also assessed in-vivo magnetic resonance imaging (MRI) of lower extremity muscles.

2 | METHODS

2.1 | Animals

All protocols were approved by the University of Maryland Institutional Animal Care & Use Committee (IACUC). The DMD rat model (Dmd-KO) was generated (by Cyagen Biosciences, Santa Clara, CA) using a clustered regularly interspaced short palindromic repeats (CRISPR)-based approach targeting exons 22–26 of dystrophin (guide RNA pairs GTCTAATAGTAGGTGATAAGAGG and CAGCT-CTTGTACCCGATTGCTGG) on the X chromosome, resulting in an out of frame deletion of exons 22–26 and a ~ 1080 bp mutant dystrophin mRNA. Four-week-old dystrophic (Dmd-KO, N = 5, 218 ± 15 g) and age-matched littermate WT (N = 5, 253 ± 17 g) male rats were used. Rats were anesthetized with isoflurane (2% with oxygen flow rate of 0.8 L/min) for in-vivo MRI and muscle testing.

2.2 | In-vivo MRI experiments

Prior to any muscle testing or injury, MRI studies were performed on a 7.0 Tesla 30-cm horizontal bore scanner (Bruker Biospec, Billerica, MA) using Paravision 6.0 software (Bruker Biospin MRI GmbH, Ettlingen, Germany). Anesthetized rats were placed supine on a holder bed and moved into the center of the magnet. After system calibration, high resolution T_2-weighted MRI images in the cross-sectional view between the hip and the knee for the thigh muscles, and between the knee and the ankle for the leg muscles, were

acquired using a rapid acquisition with relaxation enhancement (RARE) sequence with repetition time (TR)/echo time (TE) = 5000/32 ms, RARE factor = 8, field of view = 30 × 30 mm^2, matrix size = 250 × 250, slice thickness = 0.5 mm without a gap, averages = 16, number of slices = 32. Heterogeneity was quantified in bilateral thigh and leg muscles by averaging mean intensities at 3 regions of interest (ROIs) in 3 slices using ImageJ (N = 3 Dmd-KO rats, N = 2 WT rats).

2.3 | In-vivo muscle testing

We tested the quadriceps and the tibialis anterior (TA) in the left hindlimbs using established methods for testing strength and injury response (N = 5 Dmd-KO and WT rats).[13–19] Strength was assessed with the muscle at optimal length, with maximal isometric torque measured with the knee at 45° for the quadriceps and the ankle at 15° of plantarflexion for the TA.

Maximal stimulation of the target muscle in-vivo was performed as described previously.[16,18,20] Briefly, with the animal placed in a supine position, the leg (dorsiflexors) or thigh (for quadriceps) was stabilized. The axis of the ankle or knee joint, respectively, was aligned with the axis of the stepper motor (model T8904, NMB Technologies, Chatsworth, CA) and a torque sensor (QWFK-8 M, Sensotec, Columbus, OH). The fibular nerve (for dorsiflexors) or femoral nerve (for quadriceps) was stimulated via subcutaneous needle electrodes (J05 Needle Electrode Needles, 36BTP, Jari Electrode Supply, Gilroy, CA). With subcutaneous electrodes, both fibular and femoral nerves are easily accessible at the neck of the fibula and femoral triangle, respectively. Proper electrode position was determined by a series of isometric twitches and by observing isolated muscle contraction in the anesthetized animal. Maximal tetanic activation (300-ms train duration, 100 Hz) was used to assess strength.

To induce injury, we superimposed lengthening contractions onto maximal isometric contractions, using 15 repetitions through a 60° arc at 900°/s while the muscle remained stimulated, with each contraction spaced approximately 1 minute apart. A custom program based on commercial software (LabVIEW version 8.5, National Instruments, Austin, Texas) was used to synchronize contractile activation and the onset of forced joint rotation. Maximal isometric torque was measured before lengthening contractions and 5 min after the last lengthening contraction, and then used to calculate force deficits.

2.4 | Histology

Following MRI and contractile testing, quadriceps and TA muscles were harvested, weighed, snap frozen in liquid nitrogen, and stored at −80°C. Transverse sections were cut on a cryostat (10 μm thickness) and collected onto glass slides (Superfrost Plus; VWR, Radnor, PA). Sections were stained with hematoxylin and eosin (H&E), and immunolabeled with dystrophin (1:200, PA5–16734, Thermo Fisher Scientific, Waltham, MA; secondary antibody 1:100, 111–545–003, Jackson ImmunoResearch, West Grove, PA) for tissue evaluation. Sections were imaged using Eclipse T*i*2-E microscope (Nikon, Tokyo, Japan).

2.5 | Statistical analysis

Statistical analyses were performed using SigmaStat 3.5 (San Rafael, CA). Data are presented as mean ± SD. Statistical significance was assessed using Student's t-test, with $P < .05$. Scatter plots were produced using RStudio (RStudio: Integrated Development for R. RStudio, PBC, Boston, MA) and open source ggplot2 3.1.0 package.[21]

3 | RESULTS

T_2-weighted images of thigh and leg muscles in the axial view of WT rats were homogeneously dark with no focally hyperintense regions (Figure 1). Images of Dmd-KO rats showed heterogeneous muscle intensity, with multiple, unevenly distributed focal hyperintensities (Figure 1) typical of DMD. H&E staining from these muscles corresponded to the MRI heterogeneity, showing inflammation, varied fiber sizes, and centrally located nuclei, all markers expected in DMD muscle.

In-vivo muscle testing of the quadriceps and TA muscles showed weakness was present in both muscles in the Dmd-KO rat compared to the WT rat. Susceptibility to injury was also significantly greater in both muscles tested for the Dmd-KO rat, with loss of strength after injury approximately double that of the WT rat (Figure 2A,B).

4 | DISCUSSION

Similar to MRI outcomes in previous DMD animal models, Dmd-KO rat muscles also show heterogeneous signal intensity on T_2-weighted images. These high intensity foci, typically found in DMD and *mdx* hindlimb muscles, are linked to muscle damage, inflammation, and fatty infiltration.[22–24]

In previous studies, assessment of strength in DMD rats has been limited to whole body tests, such as the wire-hang test[10] and grip strength,[25] both of which incorporate central drive, endurance, and other parameters beyond skeletal muscle health. Here, we rigorously tested quadriceps and TA muscle function, eliminating effects of volition and behavior. Muscles of the Dmd-KO rat are weak and much more susceptible to injury, hall-marks of DMD. However, such findings will need to be assessed through-out the lifespan of the Dmd-KO rat to ensure that the muscle physiology reflects the progressive nature of the histological findings over time.

In conclusion, the Dmd-KO rat model is a suitable model for DMD, with increased T_2 hyperintensities in both thigh and leg muscles, and increased weakness and susceptibility to injury in both quadriceps and TA. The Dmd-KO rat will likely be a useful model to analyze the effect of developing therapeutics for DMD and to assess efficacy in improving skeletal muscle function. However, it must be noted that there are now several mouse and rat models that mimic the DMD phenotype; thus, findings described here for the Dmd-KO rat may be specific to this particular model.

ACKNOWLEDGMENTS

We thank Myologica LLC for graciously providing the WT and Dmd-KO rats.

Funding information

Muscular Dystrophy Association, Grant/Award Number: 577897; National Institute of Arthritis and Musculoskeletal and Skin Diseases, Grant/Award Numbers: K01AR074048, R56AR073193; UMB Institute for Clinical and Translational Research [ICTR]), Grant/Award Number: RML

Abbreviations:

CRISPR	clustered regularly interspaced short palindromic repeats
DMD	Duchenne muscular dystrophy
Dmd-KO	rat model missing dystrophin (Knocked Out)
H&E	hematoxylin and eosin
MRI	magnetic resonance imaging
RARE	rapid acquisition with relaxation enhancement
ROI	region of interest
RT	repetition time
TA	tibialis anterior
TE	echo time
WT	wild-type

REFERENCES

1. McDonald CM, Abresch RT, Carter GT, et al. Profiles of neuromuscular diseases. Duchenne muscular dystrophy. Am J Phys Med Rehabil. 1995;74(5 Suppl):S70–S92. [PubMed: 7576424]
2. Brooke MH, Fenichel GM, Griggs RC, et al. Duchenne muscular dystrophy: patterns of clinical progression and effects of supportive therapy. Neurology. 1989;39(4):475–481. [PubMed: 2927672]
3. Lovering RM, Porter NC, Bloch RJ. The muscular dystrophies: from genes to therapies. Phys Ther. 2005;85(12):1372–1388. [PubMed: 16305275]
4. Chamberlain JS, Metzger J, Reyes M, Townsend D, Faulkner JA. Dystrophin-deficient mdx mice display a reduced life span and are susceptible to spontaneous rhabdomyosarcoma 3. FASEB J. 2007;21(9): 2195–2204. [PubMed: 17360850]
5. Glesby MJ, Rosenmann E, Nylen EG, Wrogemann K, Serum CK. Calcium, magnesium, and oxidative phosphorylation in mdx mouse muscular dystrophy 1. Muscle Nerve. 1988;11(8):852–856. [PubMed: 3173410]
6. Muntoni F, Mateddu A, Marchei F, Clerk A, Serra G. Muscular weakness in the mdx mouse 2. J Neurol Sci. 1993;120(1):71–77. [PubMed: 8289081]
7. Dangain J, Vrbova G. Muscle development in mdx mutant mice 1. Muscle Nerve. 1984;7(9):700–704. [PubMed: 6543918]
8. Allamand V, Campbell KP. Animal models for muscular dystrophy: valuable tools for the development of therapies. Hum Mol Genet. 2000;9(16):2459–2467. [PubMed: 11005802]
9. Larcher T, Lafoux A, Tesson L, et al. Characterization of dystrophin deficient rats: a new model for Duchenne muscular dystrophy. PLoS One. 2014;9(10):e110371. [PubMed: 25310701]
10. Nakamura K, Fujii W, Tsuboi M, et al. Generation of muscular dystrophy model rats with a CRISPR/Cas system. Sci Rep. 2014;4:5635. [PubMed: 25005781]

11. Robertson AS, Majchrzak MJ, Smith CM, et al. Dramatic elevation in urinary amino terminal titin fragment excretion quantified by immunoassay in Duchenne muscular dystrophy patients and in dystrophin deficient rodents. Neuromuscul Disord. 2017;27(7):635–645. [PubMed: 28554556]
12. Morgan J, Partridge T. Skeletal muscle in health and disease. Dis Model Mech. 2020;13(2):dmm042192.
13. Pratt SJ, Lovering RM. A stepwise procedure to test contractility and susceptibility to injury for the rodent quadriceps muscle. J Biol Method. 2014;1(2):e8. 10.14440/jbm.2014.34.
14. Pratt SJ, Shah SB, Ward CW, Inacio MP, Stains JP, Lovering RM. Effects of in vivo injury on the neuromuscular junction in healthy and dystrophic muscles 1. J Physiol. 2013;591(Pt 2):559–570. [PubMed: 23109110]
15. Sanchez B, Iyer SR, Li J, et al. Non-invasive assessment of muscle injury in healthy and dystrophic animals with electrical impedance myography. Muscle Nerve. 2017;56:E85–E94. [PubMed: 28056487]
16. Lovering RM, De Deyne PG. Contractile function, sarcolemma integrity, and the loss of dystrophin after skeletal muscle eccentric contraction-induced injury. Am J Physiol Cell Physiol. 2004;286(2): C230–C238. [PubMed: 14522817]
17. Lovering RM, Roche JA, Bloch RJ, De Deyne PG. Recovery of function in skeletal muscle following 2 different contraction-induced injuries. Arch Phys Med Rehabil. 2007;88(5):617–625. [PubMed: 17466731]
18. Lovering RM, Roche JA, Goodall MH, Clark BB, McMillan A. An in vivo rodent model of contraction-induced injury and non-invasive monitoring of recovery 1. J Vis Exp. 2011;51:2782.
19. Xu S, Pratt SJ, Spangenburg EE, Lovering RM. Early metabolic changes measured by 1H MRS in healthy and dystrophic muscle after injury. J Appl Physiol. 2012;113(5):808–816. [PubMed: 22744967]
20. Iyer SR, Valencia AP, Hernandez-Ochoa EO, Lovering RM. In vivo assessment of muscle contractility in animal studies. Methods Mol Biol. 2016;1460:293–307. [PubMed: 27492180]
21. Wickham H Elegant Graphics for Data Analysis. New York, NY: Springer-Verlag; 2016.
22. Walter G, Cordier L, Bloy D, Sweeney HL. Noninvasive monitoring of gene correction in dystrophic muscle. Magn Reson Med. 2005;54(6):1369–1376. [PubMed: 16261578]
23. McMillan A, Shi D, Pratt SJP, Lovering RM. Diffusion tensor MRI to assess damage in healthy and dystrophic skeletal muscle after lengthening contractions. J Biomed Biotechnol. 2011;2011:970726. [PubMed: 22190860]
24. McIntosh LM, Baker RE, Anderson JE. Magnetic resonance imaging of regenerating and dystrophic mouse muscle. Biochem Cell Biol. 1998; 76(2–3):532–541. [PubMed: 9923723]
25. Ouisse LH, Remy S, Lafoux A, et al. Immunophenotype of a rat model of Duchenne's disease and demonstration of improved muscle strength after anti-CD45RC antibody treatment. Front Immunol. 2019;10:2131. [PubMed: 31552055]

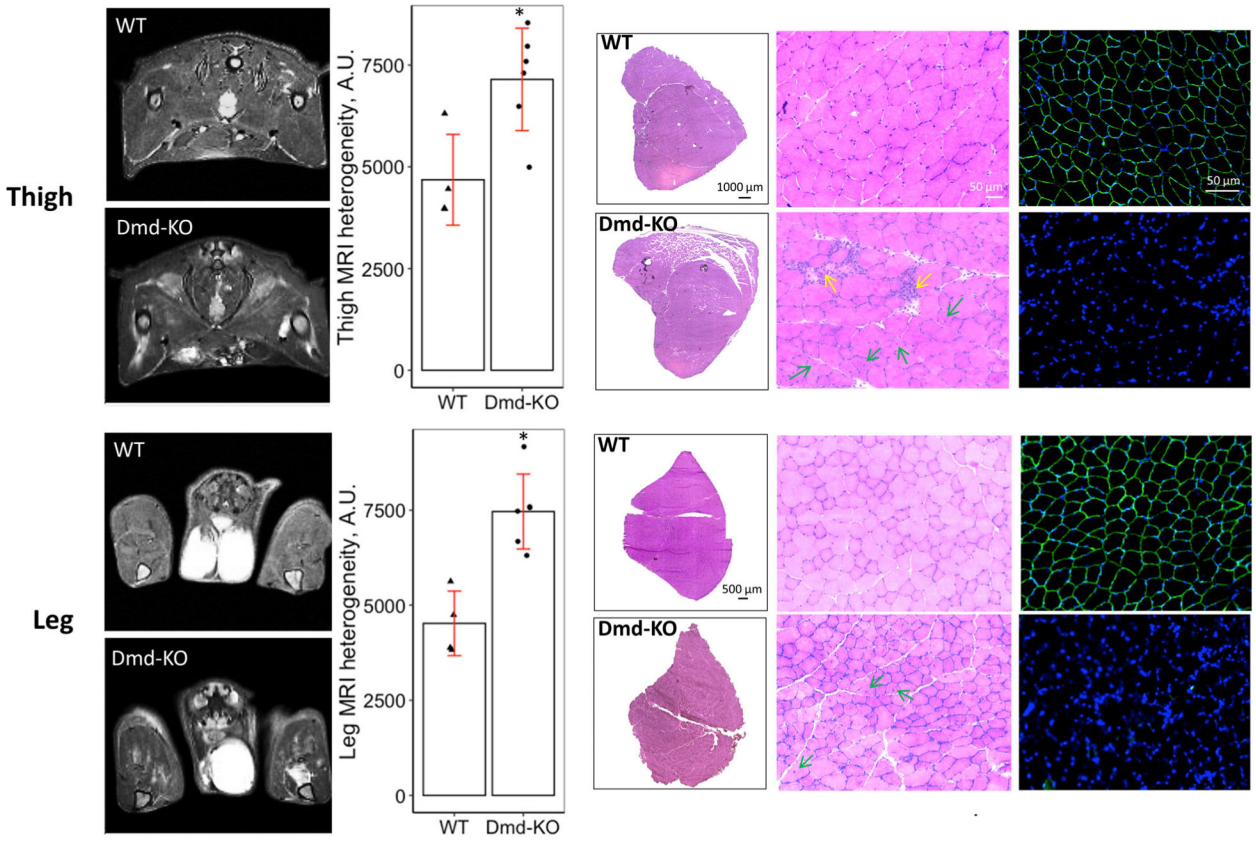

FIGURE 1.

T_2-weighted images show the thigh and leg muscles in cross-sections (axial, transverse plane) in WT and Dmd-KO rats. As noted in the Methods, imaging was performed prior to any contractile testing. Dmd-KO rat muscles have increased T_2 signal, heterogeneity, and localized hyperintensities, which have been linked to muscle damage, inflammation, and fatty infiltration. Bar graphs show heterogeneity quantification of the MRI. H&E micrographs on the left show stitched images of the entire muscle for quadriceps and TA (muscle shown are from the untested side to eliminate effects of contractile testing/injury). H&E micrographs on the right show higher power representative images of muscle tissue in cross section. WT muscles show congruent muscle fibers with relatively similar size, while Dmd-KO muscle show variability in fiber size, inflammation (yellow arrows), and centrally nucleated fibers (green arrows), a marker of ongoing muscle degeneration/regeneration. The immunofluorescent micrographs show labeling for dystrophin (green) and nuclei (blue), with absence of dystrophin in Dmd-KO muscles. A.U. = arbitrary units; * = significance at $P < .05$

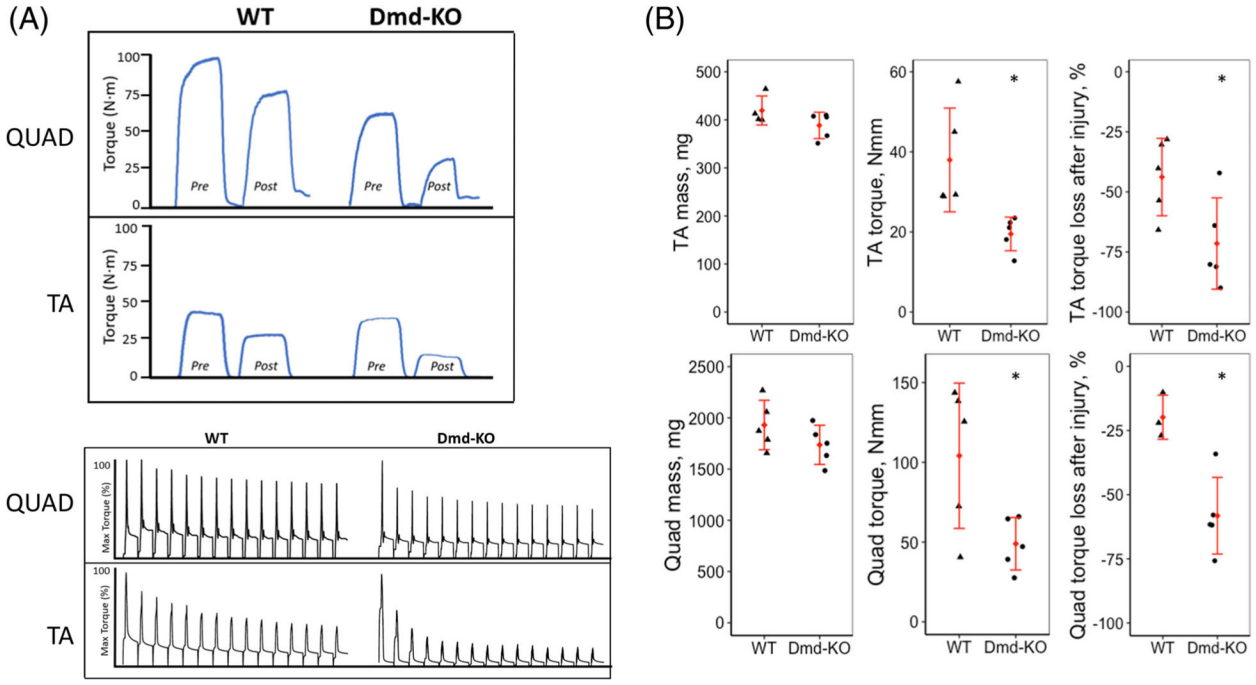

FIGURE 2.

A, The top panel shows representative curves of maximal isometric torque (200 ms in duration) before injury (pre) and after injury (post) for quadriceps (QUAD) and TA muscle of WT and Dmd-KO rats. The bottom panels show representative trace recordings of torque from lengthening (eccentric) contractions. Muscles were stimulated for 200 ms to induce a peak isometric contraction before lengthening by movement of knee (QUAD) or ankle (TA) in the opposite direction of muscle's action at that joint. **B,** Scatter plots describing muscle mass, maximal isometric torque, and susceptibility to injury for TA (top) and Quad (bottom) in WT and Dmd-KO rats. * = Significance at $P < .05$